Notch-1 signalling requires ligand-induced proteolytic release of intracellular domain

Eric H. Schroeter, Jeffrey A. Kisslinger & Raphael Kopan

Division of Dermatology and the Department of Molecular Biology and Pharmacology, Washington University, Box 8123, 4940 Parkview Place, St Louis, Missouri 63110, USA

Notch proteins are ligand-activated transmembrane receptors involved in cell-fate selection throughout development[1–3]. No known enzymatic activity is contained within Notch and the molecular mechanism by which it transduces signals across the cell membrane is poorly understood. In many instances, Notch activation results in transcriptional changes in the nucleus through an association with members of the CSL family of DNA-binding proteins (where CSL stands for CBF1, Su(H), Lag-1)[1–4]. As Notch is located in the plasma membrane and CSL is a nuclear protein, two models have been proposed to explain how they interact (Fig. 1). The first suggests that the two interact transiently at the membrane[1,5–7]. The second postulates that Notch is cleaved by a protease, enabling the cleaved fragment to enter the nucleus[6,8–14]. Here we show that signalling by a constitutively active membrane-bound Notch-1 protein requires the proteolytic release of the Notch intracellular domain (NICD), which interacts preferentially with CSL. Very small amounts of NICD are active, explaining why it is hard to detect in the nucleus *in vivo*. We also show that it is ligand binding that induces release of NICD.

Earlier work showed that Notch is proteolytically cleaved[13]. To determine whether this cleavage is essential for Notch-1 signalling, we identified and mutated the cleavage site to alter Notch-1 processing. To generate enough NICD for sequencing, we over-expressed a version of constitutively activated membrane-bound Notch-1 ($N^{\Delta E}$) (see Fig. 2a and Methods) in 10T1/2 cells using a Sindbis virus expression vector[15]. The two bands of lower relative molecular mass (Fig. 2b) were purified and subjected to ten cycles of amino-terminal sequencing. The amino-acid sequence VLLSRKRRRQHG was obtained from both bands, indicating that NICD is generated as a result of proteolytic cleavage between amino acids G1743 and V1744 (Fig. 2a). The difference in the size of the two bands is explained by the observation that NICD seems to be modified after cleavage (Fig. 2b), probably by phosphorylation (E.H.S. and R.K., unpublished observations). The sequence surrounding

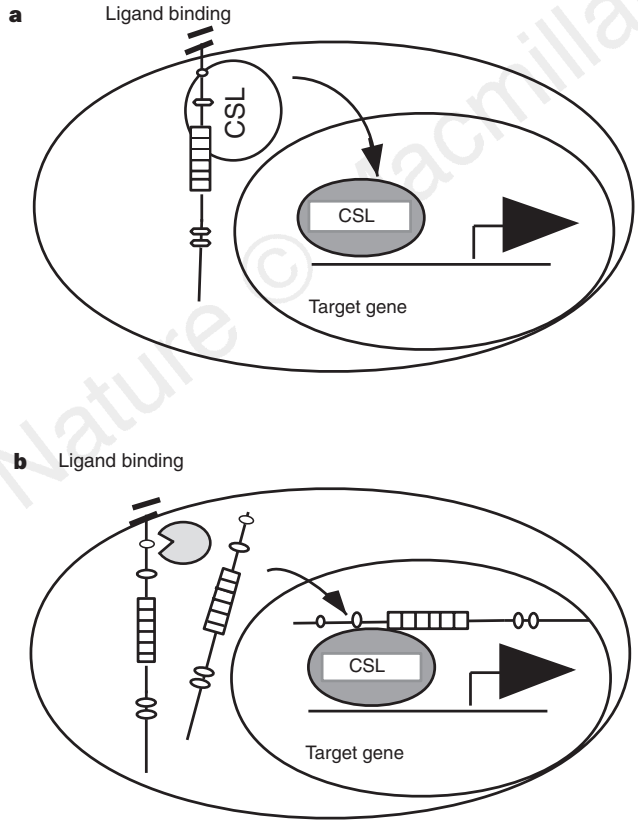

Figure 1 Different predictions are made by two models of Notch signalling. **a**, Models not invoking processing propose that interactions between Notch and CSL at the membrane may be sufficient to transduce a signal. Thus, ligand-regulated NICD release is not expected to be necessary for signalling. **b**, The processing model suggests that Notch signalling requires the release of NICD, which is capable of direct interaction with CSL in the nucleus, to turn on transcription of target genes. This model predicts that NICD release is regulated by ligand binding and that blocking proteolysis interferes with signalling. Notch-1 domain symbols as in Fig. 2.

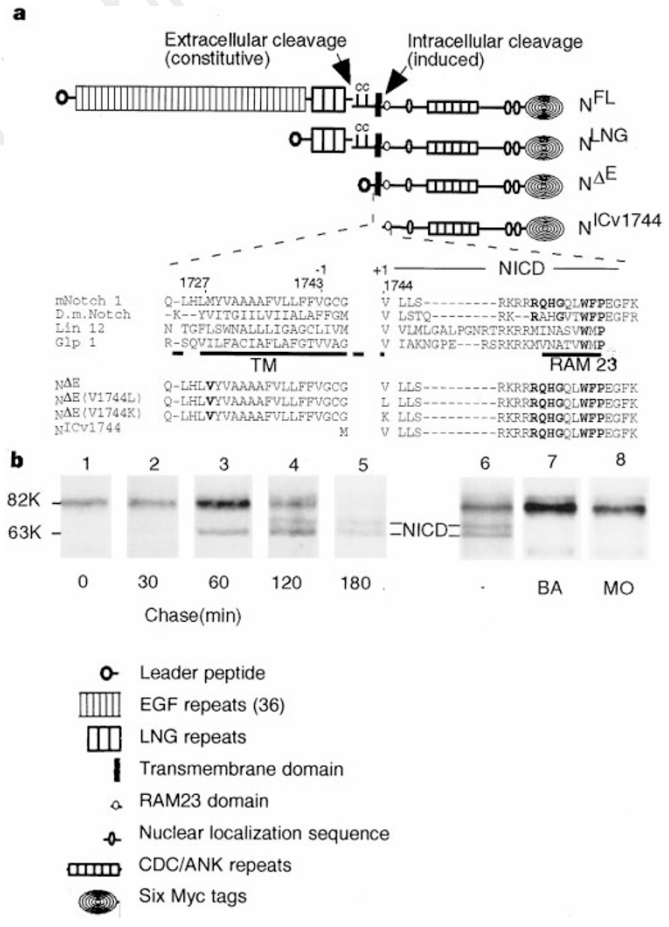

Figure 2 The Notch-1 constructs used and processing of $N^{\Delta E}$ to produce NICD. **a**, Map of domains and cleavage sites found in Notch-1 constructs used in this study. Cleavage occurs at or near the transmembrane domain (TM) between G1743(–1) and V1744(+1) (PIR entry A46019 (www-nbrf.georgetown.edu/pir/)). EGF, epidermal growth factor. M, murine; D.M., *Drosophila melanogaster*. **b**, Characterization of $N^{\Delta E}$ cleavage and release of NICD. Both lower bands in lanes 4–6 have the same N-terminal end and both represent NICD. Pulse-chase analysis shows that the lower band is produced first; a form with higher relative molecular mass appears later (lanes 3–5). Processing is inhibited by brefeldin A (BA; lane 7) and monensin (MO; lane 8), indicating that cleavage occurs after passage through the *trans*-Golgi network. Lane 6, untreated control.

G1743 and V1744 has no identity with known protease sites. Furthermore, V1744 seems to be conserved in all known Notch proteins and resides within or very close to the cytoplasmic side of the transmembrane domain (Fig. 2a).

Cleavage of Notch-1 to produce NICD is inhibited by brefeldin A (Fig. 2b, lane 7), which disassembles the Golgi apparatus[16,17], and by monensin (Fig. 2b, lane 8), which prevents transfer of proteins from the Golgi to the plasma membrane[18,19]. Thus, proteolytic release of NICD apparently occurs after export of Notch-1 from the Golgi and may take place at the plasma membrane or after internalization of membrane-bound Notch-1 protein. Kuzbanian (Kuz), an ADAM family protease[20–22], has been proposed to mediate cleavage of Notch-1 at or near a previously identified site in the extracellular domain[13] (Fig. 2a). However, this constitutive cleavage is monensin-resistant and may take place as part of the maturation of Notch in the secretory pathway[23]. In addition, dominant-negative Kuz[20] does not affect NICD release or $N^{\Delta E}$ activity in our system (data not shown), indicating that the cleavage releasing NICD is unlikely to be mediated by Kuz.

Notch signalling can initiate expression of the repressor HES-1. We tested the importance of proteolysis for Notch1-mediated regulation of the HES-1 promoter by mutating V1744 (Fig. 2a). If proteolysis is necessary for Notch-1 activity, mutations that alter cleavage of Notch-1 should correspondingly alter its activity. We evaluated effects on transcription by measuring steady-state levels of luciferase expressed from the HES-1 promoter over a range of concentrations of Notch-1 plasmid DNA in transiently transfected 3T3 cells. $N^{\Delta E(V1744)}$ mutants show a reduction in the amount of NICD produced and a parallel reduction in activity (Fig. 3a, lanes 6–8; Fig. 4a, mutants $N^{\Delta E(V1744L)}$ and $N^{\Delta E(V1744K)}$; see Methods). Differential stability is not responsible for this effect as equivalent levels of unprocessed Notch-1 protein are expressed from all mutant constructs over several different plasmid concentrations (Fig. 3a, and data not shown). As positive controls, $N^{\Delta E}$ and a construct in which V1744 becomes the first amino acid following the initiating methionine ($N^{ICV1744}$) were transfected. An inactive Notch-1 protein containing LNG repeats (Fig. 2a, N^{LNG})[13] was a negative control. Although $N^{\Delta E(V1744)}$ mutant proteins that are poorly processed have significant activity at 10 ng of plasmid, $N^{\Delta E}$ produces the same level of activity at much lower concentrations (Fig. 4a).

These results implicate NICD as the activator of HES-1 expression. However, it is possible that the effect of V1744 mutations on Notch-1 activity may be independent of cleavage. If this is true, nuclear Notch-1 proteins containing the V1744 mutations should also have reduced activity. V1744 mutant proteins that lack the transmembrane domain ($N^{IC(V1744L)}$ and $N^{IC(V1744K)}$) perform as well as $N^{\Delta E}$ and $N^{ICV1744}$ in activation of the HES-1 promoter (Fig. 4b). These results establish that Notch-1 proteins with mutations of V1744 only exhibit reduced activity when membrane-bound (Fig. 4).

The attenuation of $N^{\Delta E}$ activity caused by cleavage mutations indicates the importance of proteolysis in Notch signalling. However, V1744 is located only seven amino acids away from the conserved RAM23 site (Fig. 2a) required for *in vitro* binding of Notch to CSL[6,12,14]. This proximity raises the concern that these mutations may interfere with interactions between Notch and CSL at the membrane. We therefore examined the ability of the CSL protein RBP3[11] (CSL^{RBP3}) to bind forms of $N^{\Delta E}$ in which the cleavage site was altered. In tissue culture cells, CSL^{RBP3} precipitates equally

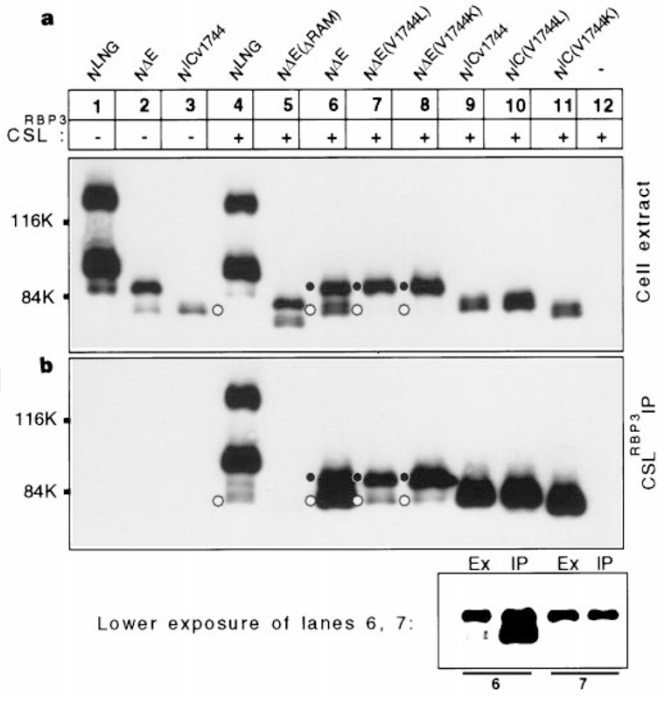

Figure 3 Western blot analysis. **a**, Equivalent amounts of unprocessed $N^{\Delta E}$ and $N^{\Delta E(V1744)}$ mutant proteins (filled circles) are detected (lanes 2, 6–8). In $N^{\Delta E(V1744)}$ mutants, production of NICD (open circles, lanes 7, 8) is greatly reduced. **b**, Notch-1 precipitated together with SL^{RBP3} from extracts used in (**a**). $N^{\Delta E}$ and $N^{\Delta E(V1744)}$ mutants all precipitate with equal efficiency (lanes 6–8, filled circles); however, NICD is enriched (open circles and inset). $N^{ICV1744}$ and its mutants all precipitate with equal efficiency (lanes 9, 10). Notch-1 is not precipitated in the absence of Flag–CSL^{RBP3} (lanes 1–3) or when the RAM23 domain is deleted (lane 5). No cross-reactivity to Myc is found in the absence of tagged Notch-1 (lane 12). IP, immunoprecipitate; Ex, extract.

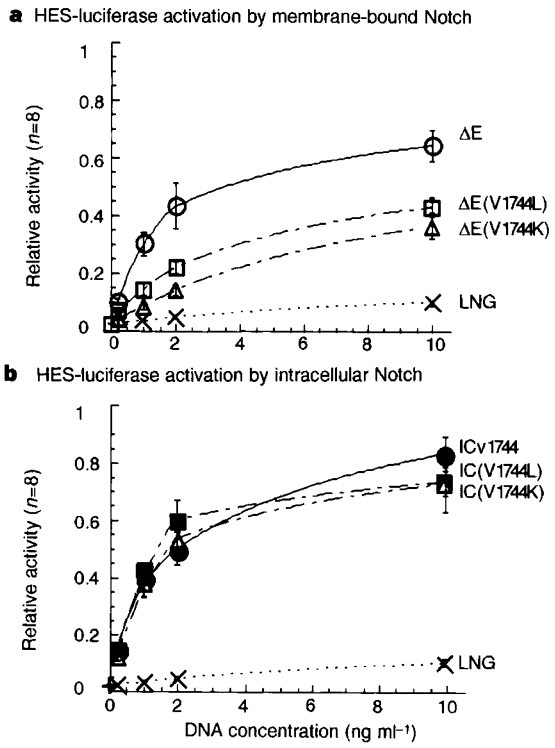

Figure 4 Activation of HES-1–luc by Notch-1 proteins. **a**, The mutant $N^{\Delta E(V1744)}$ molecules activate the HES-1 promoter at a significantly slower rate and reach <60% of the maximum activity of $N^{\Delta E}$. This level of activity (60% of maximum) is reached by $N^{\Delta E}$ at tenfold lower DNA concentration. **b**, $N^{ICV1744}$ and its mutants all accumulate luciferase at an equal rate and have the same maximum activity. Data are normalized as percentage of the activation seen with 100 ng ml^{-1} of $N^{ICV1744}$ plasmid DNA, and the results are averaged for each data point ($n = 8$). Standard errors are shown.

with the membrane-bound fraction of all $N^{\Delta E}$ proteins (Fig. 3a, b, lanes 6–8, dark dots). The same is found for all the $N^{ICV1744}$ constructs (Fig. 3a, b; lanes 9–11). Significantly, CSL^{RBP3} preferentially interacts with NICD in these cell extracts. Although only a small fraction of $N^{\Delta E}$ is processed, most of the protein precipitated with CSL^{RBP3} corresponds to NICD (Fig. 3, inset). Similar enrichment of NICD is seen with the $N^{\Delta E(V1744)}$ mutants. The amounts of NICD produced in cells expressing these proteins correlates with their activity, as follows: $N^{ICV1744} > N^{\Delta E} > N^{\Delta E(V1744K)} \geq N^{\Delta E(V1744L)} > N^{LNG}$.

Although CSL proteins do not appear to localize with Notch together in the cytoplasm *in vivo*[24,25], transient interactions may be occurring at the membrane. However, CSL preferentially binds NICD in transfected cells (Fig. 3a, b, lanes 6–8), whereas *in vitro*-translated $N^{ICV1744}$ and $N^{\Delta E}$ interact with CSL^{RBP3} with comparable affinity (not shown). Moreover, DNA-binding N^{IC}/CSL^{RBP3} complexes are found in nuclear extracts[11]. These results indicate that processing of Notch-1 at V1744 is required to release an intracellular fragment to the nucleus, where the fragment acts with CSL to activate transcription. Inhibiting this step with mutations affects their activity.

The $N^{\Delta E(V1744)}$ mutants and N^{LNG} do exhibit some activity. Therefore NICD must act at very low nuclear concentrations. To study this possibility, we first estimated how much protein is produced from $pCS2^+$ expression vectors by titrating $pCS2^+$ β-galactosidase DNA over a range of concentrations. β-Galactosidase protein accumulates linearly as a function of $pCS2^+$ DNA concentration (Fig. 5a). From 0.2 to 2 ng ml^{-1} of DNA, we detect 0.2–2 pg β-galactosidase protein per extract. These values are just above detectable levels in this assay. The HES-1 promoter, however, responds logarithmically, saturating at concentrations above 10 ng ml^{-1} $pCS2^+$ $N^{ICV1744}$ DNA (Figs 4b and 5a). This implies that by the time that detectable amounts of $N^{ICV1744}$ have accumulated, the response to $N^{ICV1744}$ has already occurred and is at >50% of saturation.

Next we estimated amounts of NICD required in single cells to produce a response from a HES-1–β-galactosidase reporter. Activation of this reporter occurred at concentrations below our Notch-1 detection level. Accumulation of $N^{ICV1744}$ protein was monitored by antibody staining in transiently transfected cells over a range of $pCS2^+$ $N^{ICV1744}$ DNA concentrations. At the same time, HES-1 promoter activity was scored by staining for β-galactosidase (Fig. 5). To increase the sensitivity of Notch-1 detection, the OPA/PEST domains were replaced with six Myc tags[13]. Using the anti-Myc antibody 9E10, $N^{ICV1744}$ can be detected at DNA concentrations starting at 2 ng ml^{-1}, indicating that detection by this antibody is similar in sensitivity to the enzymatic assay used for β-galactosidase. The number of cells expressing HES-1–β-galactosidase increases as the $pCS2^+$ $N^{ICV1744}$ DNA concentration increases (Fig. 5b). However, $N^{ICV1744}$ at a concentration of 2 ng ml^{-1} is detected in only 2% of the immunoreactive cells and no $N^{ICV1744}$ is found in the cells receiving less $pCS2^+$ $N^{ICV1744}$ DNA (Fig. 5b, d). It is only at higher Notch-1 DNA concentrations (20–100 ng; Fig. 5b, e) that most HES-1–β-galactosidase positive cells express detectable amounts of $N^{ICV1744}$ protein. Moreover, even at these higher DNA concentrations, cells expressing only β-galactosidase are found in numbers significantly higher than background (Fig. 5b). These cells must also be expressing undetectable levels of Notch-1. These data confirm that the activation threshold of the HES-1 promoter is at very low nuclear concentrations of Notch-1 and may explain why nuclear NICD has not been detected by antibodies in developing tissues.

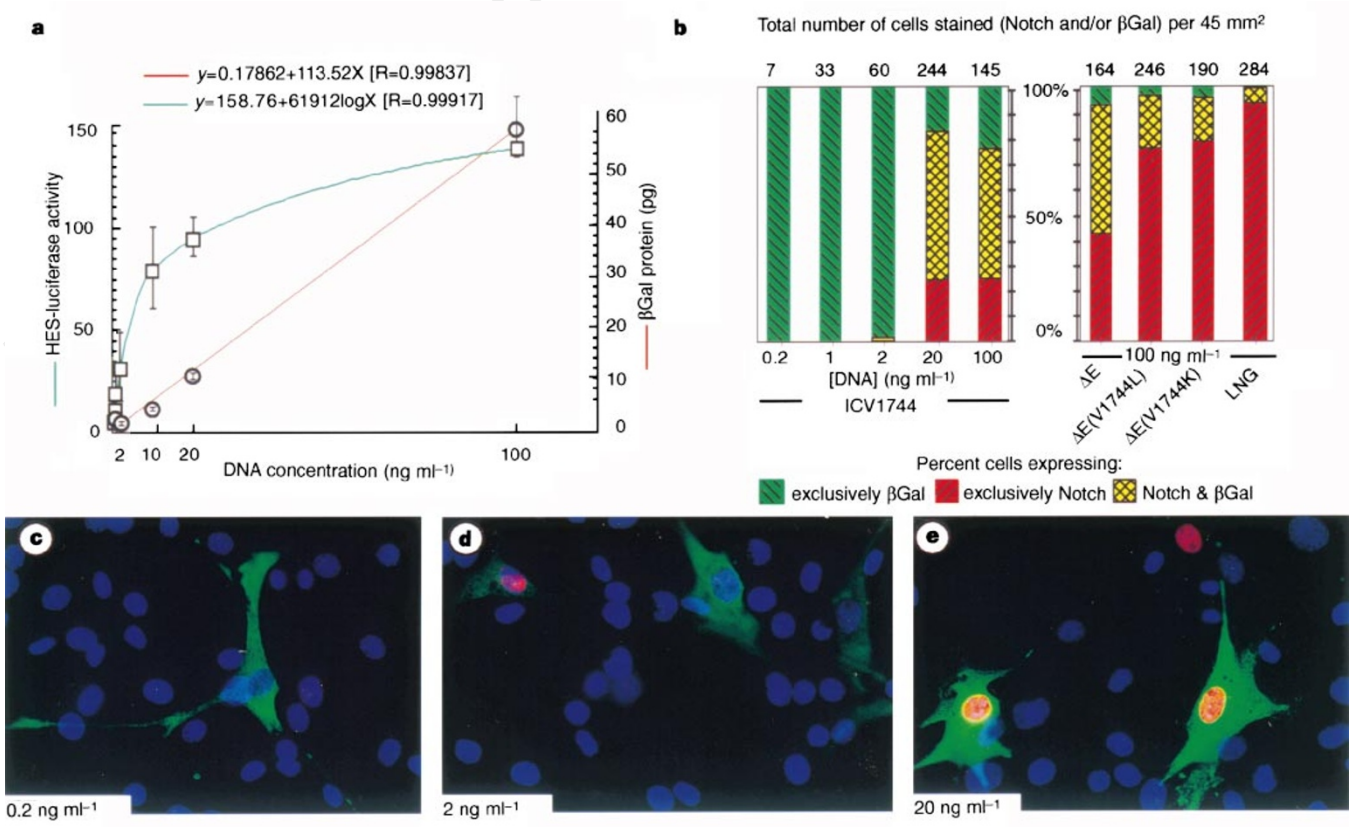

Figure 5 Notch-1 acts below threshold of detection. **a**, Production of β-galactosidase (βGal) protein from the $pCS2^+$ vector is linear. Production of $N^{ICV1744}$ from $pCS2^+$ induces a logarithmic response from the HES-1 promoter. **b**, $pCS2^+$ $N^{ICV1744}$ titrated in the presence of the HES-1–βGal reporter, monitored by immunofluorescence. Total nunbers of stained cells (~20,000 scanned) are shown above each bar. The threshold of HES-1 activation is lower than the threshold of detection of Notch-1. The percentage of βGal-positive cells decreases in cells expressing mutant $N^{\Delta E(V1744)}$ or N^{LNG}. **c**–**e**, High-magnification view of $N^{ICV1744}$ transfected cells described in (**b**). Red, Notch-1; green, βGal; blue, nuclei.

Cells expressing $N^{\Delta E(V1744)}$ mutants have the same overall levels of Notch-1 protein as do cells expressing $N^{\Delta E}$ but differ in the amount of NICD produced and the degree of HES-1 activation (Figs 3a and 4a). This could result either from lower HES-1 reporter activation in the same number of cells, or from maximal activation of the HES-1 reporter in fewer cells. At saturating DNA concentrations, half as many cells transfected with $N^{\Delta E(V1744)}$ mutants as cells transfected with $N^{\Delta E}$ express the HES-1–β-galactosidase reporter (yellow and green bars, Fig. 5b). These data support the proposal that an increase in NICD concentration increases the probability of forming fully functional transcription complexes at the HES-1 promoter, rather than increasing the rate of transcription from a fixed number of templates[26]. The mutations decrease this probability by decreasing the amounts of NICD produced.

The processing model predicts that ligand binding of full-length Notch-1 should result in NICD release. Such cleavage has not been observed previously by western blot analysis or immunohistochemistry (Fig. 6a). As immunoprecipitaiton of CSL^{RBP3} enriches for NICD, we used this technique to test whether the Notch-1 ligand Jagged-1[27] can induce cleavage of N^{FL} (see Methods) in tissue culture cells. In all experiments, a cleaved product that migrates together with NICD is upregulated when N^{FL} is transfected with the ligand Jagged-1 (Fig. 6b). To confirm the identity of this cleaved product as NICD, N^{FL} proteins containing cleavage mutations ($N^{FL(V1744L)}$ and $N^{FL(V1744K)}$) were also transfected with Jagged-1. In these experiments, no cleavage was observed (Fig. 6b). Thus, ligand binding can induce proteolytic processing of Notch-1 at V1744, releasing NICD.

In conclusion, activation of CSL by Notch-1 in vertebrate cells requires processing and nuclear localization of Notch-1, and V1744 is essential for efficient processing to occur. This same mechanism may also be vital in Notch-mediated oncogenesis[28]. In addition, very low levels of NICD are enough to produce a significant response. Such low levels of NICD can be detected by co-precipitation with Flag–CSL^{RBP3} and, significantly, NICD can be found in cells following interaction between Notch-1 and Jagged-1. Ligand-mediated processing of a membrane-bound transcription factor has also been demonstrated for the sterol regulatory-element-binding protein[29], which, unlike Notch, binds DNA directly. It is unknown whether processing is required for CSL-independent signalling events and whether processing of other Notch proteins occurs. □

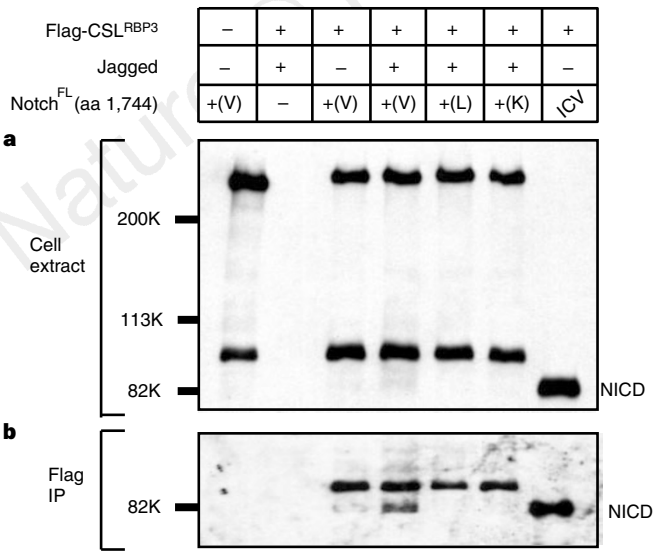

Figure 6 Full-length Notch-1 is cleaved when expressed together with Jagged-1. N^{FL}, CSL^{RBP3} and Jagged-1 were all expressed in kidney epithelial 293 cells, which allow high transfection efficiency and cell–cell contact. *In vivo*, ligand and receptor are often expressed in the same cell, but Notch activation results from ligand presented by one cell to Notch on another cell[1]. Notch-1 was co-precipitated as in Fig. 3. NICD is markedly upregulated when N^{FL} is transfected with Jagged-1 and is absent in the processing mutants $N^{FL(V1744L)}$ and $N^{FL(V1744K)}$. Transfection of full-length Notch-1 and CSL^{RBP3} alone does not generate similar fragments. **a**, Whole-cell extract. **b**, Immunoprecipitation (IP) with Flag. +(V), +(L), +(K) and the V of ICV indicate the amino acid at position 1,744 of N^{FL}.

Methods

Plasmids. Proteins were expressed using the vector $pCS2^{+}$[30]. $N^{\Delta E}$[13], N^{LNG}[13], pCS2+ β-galactosidase[30], HES-1-luc″, Flag-$CSL^{RBP3''}$ and Jagged-1[27] have been described. $N^{\Delta E}$ has the methionine at position 1,727 replaced with a valine[13]. $pCS2^{+}$ $N^{\Delta E(\Delta RAM)}$ is an in-frame deletion of amino acids 1,751–1,778. $pCS2^{+}$ N^{FL} contains the Notch-1 protein up to amino acid 2,813, fused to a hexameric Myc tag at the carboxy terminus. $pCS2^{+}$ luc contains the *Hin*dIII to *Sal*I luciferase-coding fragment of pGL2-basic ligated in $pCS2^{+}$ cut by *Hin*dIII/*Xho*I.

We mutated the $N^{\Delta E}$ processing site by amplifying two overlapping polymerase chain reaction (PCR) products. The outside primers RR66 (5′-CCCAAGCTTGATTTAGGTGAC-3′) and M95 (5′-TCGAACATTGACATCC ATGCA-3′) were used with appropriate inside primers containing mutations to form primary PCR products. Secondary PCR products were purified, digested with *Hin*dIII and *Msc*I and ligated into the same sites in $N^{\Delta E}$. Primers used for mutagenesis at V1744 were TGTGGGCTGTGGGnnnCTGCTGT CCCGCAA and TTGCGGGACAGCAGnnnCCCACAGCCCACA, with nnn representing the mutagenized codons CTG (in V1744L) and AAA (in V1744K). A *Not*I fragment containing the mutations were then moved into $pCS2^{+}$ N^{FL} to make $pCS2^{+}$ $N^{FL(V1744L)}$ and $pCS2^{+}$ $N^{FL(V1744K)}$. To create $pCS2^{+}$ $N^{ICV1744}$ and its mutants, the primer CCAGGATCCACCATGnnnCTGCTGTCCCGCAAGC was synthesized. This primer was used with M95 to generate a product that was digested with *Bam*HI and *Bcl*I, and ligated into the same sites in $N^{\Delta E}$. GTG was used for the V1744 codon.

Transfection and reporter gene assays. 3T3 cells were cultured in Dulbecco's modified Eagle's medium (DMEM) supplemented with 10% bovine calf serum. 10T1/2 and 293T cells were cultured in DMEM supplemented with 10% fetal bovine serum. Notch-1 activity was determined by measuring luciferase activity in 3T3 cells following transient transfection with HES-1–luc[11]. Transfections were performed as described[13] except that volumes were scaled down to produce 2 ml of medium in a 6-well dish. Each well was transfected with a total of 2 μg DNA consisting of: 400 ng HES-1–luc, 40 ng $pCS2^{+}$ β-galactosidase, 0.4–400 ng $pCS2^{+}$ Notch-1, with the remaining DNA made up to 2 μg with empty $pCS2^{+}$ vector. 100 μl lysate was used to determine luciferase activity as described[6]. 5 μl lysate was used to determine β-galactosidase concentration and equalize results for transfection efficiency. Assays for β-galactosidase were performed using the chemiluminescent substrate Galacton (Tropix). Experiments were performed in duplicate and repeated four times. Maximal HES-1–luc activation varied between 20- and 50-fold. For immunofluorescent examination, cells were transfected as above except that HES-1–β-galactosidase was used as a reporter and $pCS2^{+}$ luc was used for equalization. Fixed and permeablized cells were incubated with the monoclonal anti-Myc antibody 9E10 and a rabbit polyclonal anti-β-galactosidase antibody (5prime3prime). BODIPY-conjugated goat anti-rabbit and Cy3-conjugated goat anti-mouse antibodies were used as secondary antibodies. Nuclei were visualized with Hoechst stain. For cell counting, one diameter (45 mm^2 area) was scanned on each plate. $pCS2^{+}$ luc controls show that transfection efficiency varied by less than twofold (not shown).

Viral expression and sequencing. A Sindbis virus expression system was used to overexpress Notch-1 protein for microsequencing. The 1,873-base-pair *Sph*I/*Sna*BI fragment of $N^{\Delta E}$ containing the coding sequence was ligated into the plasmid pSinRep5 using the *Sph*I and *Stu*I sites to make pSR/$N^{\Delta E}$. Viral particles were produced using the defective helper RNA DHBB as described[15] and used to infect ten 100-mm dishes of 10T1/2 cells. At 48 h after infection, Notch-1 was isolated and processed for microsequencing[13].

Pulse chase and drug treatments. Subconfluent monolayers of 10T1/2 cells were infected with SR/$N^{\Delta E}$ pseudovirions and used 24 h after infection. Brefeldin A was prepared as a 1 mg ml^{-1} stock in methanol and used at a concentration of 2 μg ml^{-1}. Monensin was prepared as a 10 mM stock in ethanol and used at a concentration of 10 μM. Labelling experiments and

immunoprecipitations were done as described[13]. Ethanol and methanol controls did not alter processing.

Co-precipitations. Notch-1 proteins were precipitated together with Flag–CSL^{RBP3} from transiently transfected 293T cells as described[7], with the following modifications: anti-Flag antibody M2 (Kodak) was used to precipitate Flag–CSL^{RBP3} and Myc-tagged Notch-1 proteins were detected with monoclonal antibody 9E10. Duplicate 60-mm plates were transfected with 1.5 μg Notch-1 plasmid and/or $pCS2^+$ Jagged-1 and $pCS2^+$ Flag–CSL^{RBP3} (3 μg), and $pCS2^+$ vector was added to a total of 6 μg. Cells were lysed and pooled in 1 ml buffer[7]. Notch-1 does not precipitate from cell extracts that were transfected separately with CSL^{RBP3} and Notch-1 and then mixed (data not shown).

Received 22 December 1997; accepted 22 April 1998.

1. Artavanis-Tsakonas, S., Matsuno, K. & Fortini, M. E. Notch signaling. *Science* **268,** 225–232 (1995).
2. Kopan, R. & Turner, D. The Notch pathway: democracy and aristrocracy during the selection of cell fate. *Curr. Opin. Neurobiol.* **6,** 594–601 (1996).
3. Weinmaster, G. The ins and outs of Notch signaling. *Mol. Cell. Neurosci.* **9,** 91–102 (1997).
4. Artavanis-Tsakonas, S. Alagille syndrome—a notch up for the Notch receptor. *Nature Genet.* **16,** 212–213 (1997).
5. Fortini, M. E. & Artavanis-Tsakonas, S. The suppressor of hairless protein participates in Notch receptor signaling. *Cell* **79,** 273–282 (1994).
6. Roehl, H., Bosenberg, M., Blelloch, R. & Kimble, J. Roles of the Ram and Ank domains in signaling by the *C-elegans* Glp-1 receptor. *EMBO J.* **15,** 7002–7012 (1996).
7. Aster, J. C. *et al*. Oncogenic forms of Notch1 lacking either the primary binding site for Rbp-J-kappa or nuclear localization sequences retain the ability to associate with Rbp-J-kappa and activate transcription. *J. Biol. Chem.* **272,** 11336–11343 (1997).
8. Lieber, T., Kidd, S., Alcamo, E., Corbin, V. & Young, M. W. Antineurogenic phenotypes induced by truncated Notch proteins indicate a role in signal transduction and may point to a novel function for Notch in nuclei. *Genes Dev.* **7,** 1949–1965 (1993).
9. Kopan, R., Nye, J. S. & Weintraub, H. The intracellular domain of mouse Notch: a constitutively activated repressor of myogenesis directed at the basic helix-loop-helix region of MyoD. *Development* **120,** 2385–2396 (1994).
10. Hsieh, J. J.-D. & Hayward, S. D. Masking of the CBF1/RBPjκ transcriptional repression domain by Epstein-Barr virus EBNA2. *Science* **268,** 560–563 (1995).
11. Jarriault, S. *et al*. Signalling downstream of activated mammalian Notch. *Nature* **377,** 355–358 (1995).
12. Tamura, K. *et al*. Physical interaction between a novel domain of the receptor Notch and the transcription factor Rbp-J-kappa/Su(H). *Curr. Biol.* **5,** 1416–1423 (1995).
13. Kopan, R., Schroeter, E. H., Weintraub, H. & Nye, J. S. Signal transduction by activated mNotch: importance of proteolytic processing and its regulation by the extracellular domain. *Proc. Natl Acad. Sci. USA* **93,** 1683–1687 (1996).
14. Wettstein, D. A., Turner, D. L. & Kintner, C. The *Xenopus* homolog of *Drosophila* Suppressor Of Hairless mediates Notch signaling during primary neurogenesis. *Development* **124,** 693–702 (1997).
15. Bredenbeek, P. J., Frolov, I., Rice, C. M. & Schlesinger, S. Sindbis virus expression vectors: packaging of RNA replicons by using defective helper RNAs. *J. Virol.* **67,** 6439–6446 (1993).
16. Fujiwara, T., Oda, K., Yokota, S., Takatsuki, A. & Ikehara, Y. Brefeldin A causes disassembly of the Golgi complex and accumulation of secretory proteins in the endoplasmic reticulum. *J. Biol. Chem.* **263,** 18545–18552 (1988).
17. Doms, R. W., Russ, G. & Yewdell, J. W. Brefeldin A redistributes residence and itinerant Golgi proteins to the endoplasmic reticulum. *J. Cell Biol.* **109,** 61–72 (1989).
18. Griffiths, G., Quinn, P. & Warren, G. Dissection of the Golgi complex. I. Monensin inhibits the transport of viral membrane proteins from medial to trans Golgi cisternae in baby hamster kidney cells infected with Semliki Forest virus. *J. Cell Biol.* **96,** 835–850 (1983).
19. Quinn, P., Griffiths, G. & Warren, G. Dissection of the Golgi complex. II. Density separation of specific Golgi functions in virally infected cells treated with monensin. *J. Cell Biol.* **96,** 851–856 (1983).
20. Pan, D. J. & Rubin, G. M. Kuzbanian controls proteolytic processing of Notch and mediates lateral inhibition during *Drosophila* and vertebrate neurogenesis. *Cell* **90,** 271–280 (1997).
21. Sotillos, S., Roch, F. & Campuzano, S. The metalloprotease-disintegrin Kuzbanian participates in Notch activation during growth and patterning of *Drosophila* imaginal discs. *Development* **124,** 4769–4779 (1997).
22. Wen, C., Metzstein, M. M. & Greenwald, I. Sup-17, a *Caenorhabditis elegans* ADAM protein related to *Drosophila* KUZBANIAN, and its role in the Lin-12/Notch signaling. *Development* **124,** 4759–4767 (1997).
23. Blaumueller, C. M., Qi, H. L., Zagouras, P. & Artavanis-Tsakonas, S. Intracellular cleavage of Notch leads to a heterodimeric receptor on the plasma membrane. *Cell* **90,** 281–291 (1997).
24. Gho, M., Lecourtois, M., Geraud, G., Posakony, J. W. & Schweisguth, F. Subcellular localization of Suppressor of Hairless in *Drosophila* sense organ cells during Notch signalling. *Development* **122,** 1673–1682 (1996).
25. Honjo, T. The shortest path from the surface to the nucleus: RBPjk/Su(H) transcription factor. *Genes Cells* **1,** 1–9 (1996).
26. Weintraub, H. Formation of stable transcription complexes as assayed by analysis of individual templates. *Proc. Natl Acad. Sci. USA* **85,** 5819–5823 (1988).
27. Lindsell, C. E., Shawber, C. J., Boulter, J. & Weinmaster, G. Jagged: a mammalian ligand that activates Notch1. *Cell* **80,** 909–917 (1995).
28. Capobianco, A. J., Zagouras, P., Blaumueller, C. M., Artavanis-Tsakonas, S. & Bishop, J. M. Neoplastic transformation by truncated alleles of human NOTCH1/TAN1 and NOTCH2. *Mol. Cell. Biol.* **17,** 6265–6273 (1997).
29. Brown, M. S. & Goldstein, J. L. The SREBP pathway—regulation of cholesterol metabolism by proteolysis of a membrane-bound transcription factor. *Cell* **89,** 331–340 (1997).
30. Turner, D. L. & Weintraub, H. Expression of achaete-scute homolog 3 in *Xenopus* embryos converts ectodermal cells to a neural fate. *Genes Dev.* **8,** 1434–1447 (1994).

Acknowledgements. We thank A. Israel for providing us with the FLAG–CSL^{RBP3} expression vector; I. Frolov for the Sindbis virus vectors pSINrep5 and DHBB; G. Rubin and D. J. Pan for the Kuzbanian cDNAs; D. Syder and M. Crankshaw for technical help; R. Cagan, I. Boime, J. Gordon, D. Ornitz and members of the Kopan lab for reading and commenting on the manuscript; and G. Goldberg, G. Grant and B. Marmer for discussions and technical advice. R. K. Thanks H. Weintraub for encouragement and support. This research was supported by the NIH.

Correspondence and requests for materials should be addressed to R.K. (e-mail: kopan@pharmdec.wustl.edu).

Transcriptional repression by the methyl-CpG-binding protein MeCP2 involves a histone deacetylase complex

Xinsheng Nan*†, Huck-Hui Ng*†, Colin A. Johnson‡, Carol D. Laherty§, Bryan M. Turner‡, Robert N. Eisenman§ & Adrian Bird*

** Institute of Cell and Molecular Biology, University of Edinburgh, Kings Buildings, Edinburgh EH9 3JR, UK*
‡ Department of Anatomy, The Medical School, University of Birmingham, Birmingham B15 2TT, UK
§ Division of Basic Sciences, Fred Hutchinson Cancer Research Center, Seattle, Washington 98104, USA
† These authors contributed equally to this work.

Cytosine residues in the sequence 5′CpG (cytosine–guanine) are often postsynthetically methylated in animal genomes. CpG methylation is involved in long-term silencing of certain genes during mammalian development[1,2] and in repression of viral genomes[3,4]. The methyl-CpG-binding proteins MeCP1 (ref. 5) and MeCP2 (ref. 6) interact specifically with methylated DNA and mediate transcriptional repression[7–9]. Here we study the mechanism of repression by MeCP2, an abundant nuclear protein that is essential for mouse embryogenesis[10]. MeCP2 binds tightly to chromosomes in a methylation-dependent manner[11,12]. It contains a transcriptional-repression domain (TRD) that can

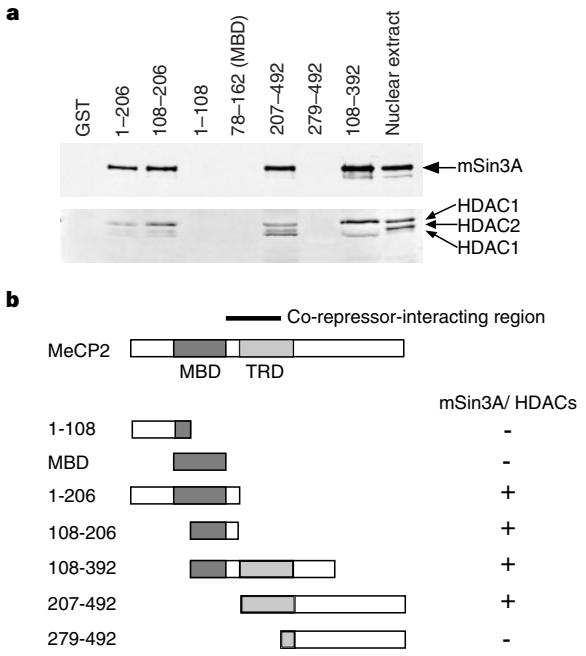

Figure 1 Interaction of MeCP2 with mSin3A and histone deacetylases. **a**, Western blot analysis of HeLa nuclear proteins pulled down by immobilized GST or by GST-fusion proteins that included different regions of MeCP2 (see **b**). Numbers correspond to amino-acid positions in the protein. Blots were probed with antibodies against mSin3A (antibody K-20), or against HDAC1 and HDAC2. The lower HDAC1 band probably corresponds to a degradation product of HDAC1. The HDAC2 band in lane 108–392 is displaced upwards because a large amount of fusion protein migrates with the HDAC2. **b**, Map of regions of MeCP2 that do (+) or do not (–) pull down mSin3A and HDACs. The thick black line corresponds to the corepressor-interacting region defined by these experiments. MBD, methyl-CpG-binding domain[11].